WALL SKIN FRICTION ASSESSMENT IN BOUNDARY LAYER FLOWS FROM THREE MEASURING TECHNIQUES

E.-S. Zanoun, L. Jehring, and C. Egbers

Department of Aerodynamics and Fluid Mechanics (LAS), BTU Cottbus,
Siemens-Halske-Ring 14, D-03046 Cottbus, Germany

ABSTRACT

The present paper aims at evaluating the wall skin friction data in laminar and turbulent boundary layer flows from three measuring techniques, namely, the Laser-Doppler anemometer (LDA) mean-velocity profile, the oil film interferometry (OFI), and the surface hot-film anemometry (HFA). A comparison among the three techniques is presented, indicating that the thermal conductivity of the substrate and glue material influence to a great deal the heat loss from the HFA. On the other hand, good agreement was observed between the wall skin friction data obtained either from the oil film interferometry or the LDA mean velocity profiles.

1. INTRODUCTION

The wall skin friction data are of vital importance in turbulence research as well as for practical applications, e.g.; see Fig. 1. The figure clarifies why there are concerns about the boundary layer investigations for wall-bounded shear flows, particularly, the wall skin friction that represents around 50% of the total drag of an airplane or 30% of ground vehicles' total drag.

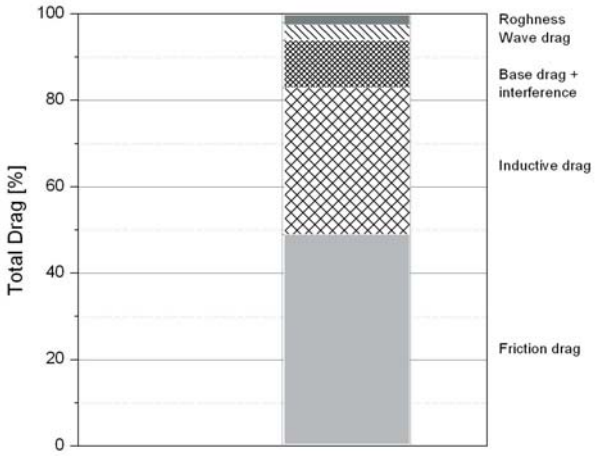

Fig. 1 Contributions of various components to the total drag of a long-range subsonic passenger airplane [1].

Hence, choosing an appropriate measuring technique for the wall skin friction measurement is a crucial issue whether it will interfere with flow or not. Utilizing the laser-Doppler anemometry and/or the oil film interferometry, for instance, are not intrusive and provide data with high enough spatial resolution. On the other hand, the hot wire/film anemometry (HWA/HFA) interferes with flow in addition to the inherent problems they have when applied in the wall vicinity because of the heat loss to the wall material. Good treatment and literature for such measuring techniques are found in [2-10].

Carrying out detailed mean velocity measurements close to the wall, in particular, when the size of the control volume (CV) of the measuring technique is small enough to resolve the laminar sublayer, represents a common base for different approaches to obtain the wall shear stress by relating the shear stress to the strain rate as follows:

$$\tau_w = -\mu (dU/dy)_w \quad (1)$$

This requires reliable velocity data within the viscous sublayer free from the wall effects; see Fig. 2, [8].

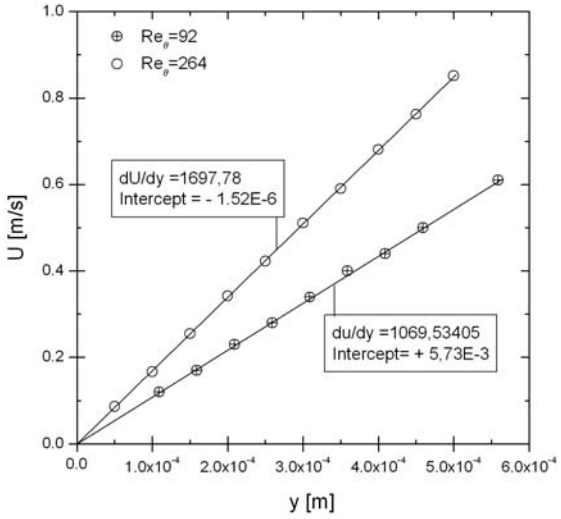

Fig. 2 The viscous sublayer mean velocity profiles for two low Reynolds numbers.

On the other hand, when the size of the CV of the measuring technique is not small enough to resolve the laminar sublayer and claiming that close to the wall a universal velocity function exists that depends only on the wall distance and the shear stress, not on flow geometry, i.e., $U = f(\tau_w, y)$, Clauser method to estimate the wall skin

friction was established [11]. Clauser method relied on the assumption that the universal velocity function extends outside the viscous sublayer, i.e., to the so-called inertial sublayer and behaving in a logarithmic manner. Therefore, in addition to the near-wall velocity measurements utilizing the LDA, the Clauser method is re-evaluated and utilized in the present study despite the fact that some questions have been recently raised about the law of the wall, whether it behaves in logarithmic or power manner, see e.g.; [12, 13], and about the constants of the former. Recent values for both constants, i.e., the von Kàrmàn and the additive constants, of the logarithmic line obtained by [12, 14] along flat plate boundary layer flows under various pressure gradients, were utilized resulting in good applicability for the Clauser plot to estimate the wall skin friction data when compared with the other measuring techniques.

NOMENCLATURE

A, B, C	Constants
a	Overheat ratio
E	Mean hot film output
T	Mean temperature
U	Streamwise mean velocity component
u_τ	Wall friction velocity
x_i	Cartesian coordinates
y	Normal wall distance

Subscripts

c	Characteristic quantities
w	wall
∞	Free stream

Superscripts

+	in wall coordinates
*	in dimensionless form

Greek letters

κ	von Kàrmàn constant
Λ	Constant ($1/\kappa$)
ρ	Fluid density
μ	Dynamic viscosity
τ	Mean wall shear stress
η	Nondimensional vertical coordinate
θ	Momentum thickness

Dimensionless Numbers

Re	Reynolds number
Gr	Grashof number
Pr	Prandtl number
Ec	Eckert number

2. EXPERIMENTAL APPARATUS AND MEASURING TECHNIQUES

2.1. Wind tunnel

The experimental work has been conducted in a low-speed wind-tunnel test facility located at the department of Aerodynamics and Fluid Mechanics (LAS), Brandenburg University of Technology (BTU), Cottbus. The tunnel has a test section of 0.6×0.5 m^2 cross-sectional area and a length of 1.8 m, see Fig. 3. It is designed for air velocities up to 50 m/s with an empty test section. The background turbulence intensity of the incident flow is less than 0.5 % in the core of the test section. Two flat plates were prepared to be separately installed inside the test section, each has dimensions of 1050×18×595 mm^3, permitting good access to the boundary layer flow. One plate was made from anodized aluminum as a highly heat-conducting wall and the other was made of glass as an adiabatic wall. The aluminum plate was anodized to yield a black non-shiny surface to avoid the unnecessary LDA-light scattering from the wall and to increase the resultant signal-to-noise ratio. The other plate was blackened from the lower side to provide a suitable surface for light reflection for the oil film interferometry. Both plates were aligned to the flow when mounted in the test section to assure zero pressure gradient boundary layer flows.

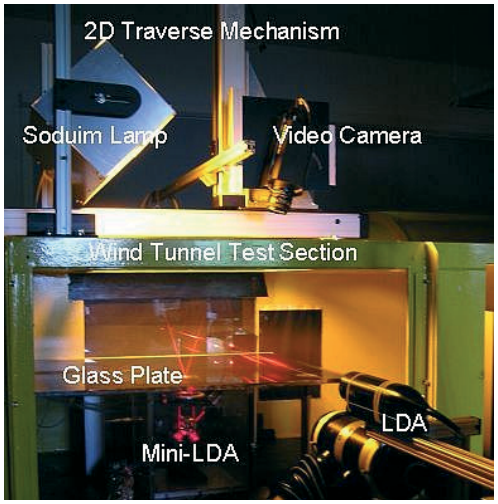

Fig. 3 Photograph of the experimental test facility showing the LDA and the optical setup for the OFI.

2.2. Laser Doppler Anemometry

A conventional one-dimensional Laser-Doppler anemometer, DANTEC Flowlite, operating in the dual-beam back-scattering mode was used to carry out the mean velocity measurements, more details can be found in [15]. The current measurements were conducted for $Re_\theta \leq 10^4$, where Re_θ is the Reynolds number based on the momentum thickness (θ) and the free stream velocity (U_∞).

2.3. Oil Film Interferometry

An alternative and more convenient technique to obtain the wall shear stress, directly, if the LDA near-wall velocity cannot be obtained precisely, is the oil-film interferometry. The basic concept of the oil film to obtain the wall shear stress, is to measure the slope of a thin oil film when displaced in a gas flow illuminated by monochromatic light, see Fig. 4.

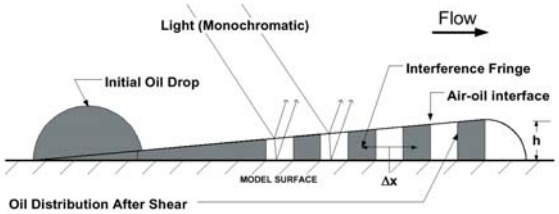

Fig. 4 Sketch illustrates the oil film intereferometry principle [16].

The variation of the thickness $h=h(x,t)$ of the thin film in two-dimensional flow is given by:

$$\frac{\partial h}{\partial t} = -\frac{1}{2\mu_o}\frac{\partial(\tau_w h^2)}{\partial x} \quad (2)$$

where h is the oil film thickness and μ_o is the oil viscosity, see, e.g.; [2, 7]. Equation (2) indicates that to obtain a value for the wall shear stress, it is necessary to measure, $h, \partial h/\partial x$ and $\partial h/\partial t$. Hence, the solution of equation (2) gives the wall shear stress:

$$\tau_w\left[\kappa + h_0/\Delta h\right] = \mu_0\, u_k\, \frac{2\left[n^2 - \sin^2\alpha\right]^{1/2}}{\lambda} \quad (3)$$

here h_0 stands for the height of the zeroth black fringe at the film edge (i.e. k=0), h_k is the height of the film at the k^{th} black fringe and Δh is the height difference between two consecutive fringes, $\Delta h = \lambda/2(n^2 - \sin^2\alpha)^{1/2}$, λ is the light wavelength, n is the refractive index of the oil and α is the camera-viewing angle. Values of μ_0, n, α and λ are usually given and from the x-t diagram, Fig. 5, an arbitrary number of fringe velocities, u_k, are measured and consequently the wall shear stress is estimated.

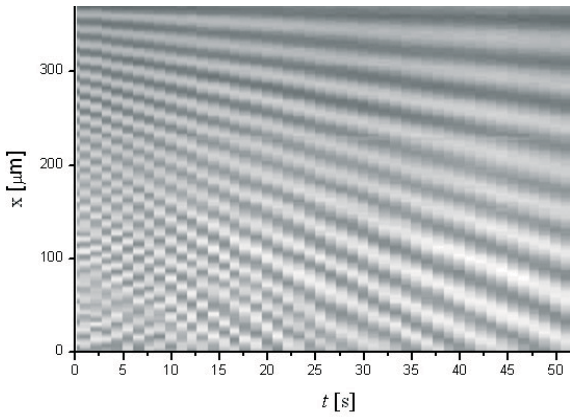

Fig. 5 The oil film thickness development over the time

The optical test setup needed for the oil film interferometry is shown in Fig. 2. It consists mainly of a gray-scale CCD camera (VCAM040 CCD-Kam Model CSB-305) with resolution of 752×582 pixels and a 30-W sodium lamp having a wavelength of 589 nm to illuminate the oil film. A 25-mm FL F/1.4 Nikkor lens was mounted with the camera in addition to a ring, i.e. lens extension 14-mm F-mount. A PCI frame grabber card, Model 600067, was used to digitize the analog output of the camera at preset time intervals. A two-dimensional traversing mechanism is also shown to facilitate the movement of the video camera to obtain well-focused images of the oil movement, see Fig. 6, and the resultant interference fringes. The angle between the camera axis and the normal direction to the glass wall forming the wall where shear stress is desired is 15° and kept constant during all measurements. The glass plate is blackened on its lower side to provide a suitable surface for light reflection.

A sequence of images (image stacks) as shown in Fig. 6 was recorded together with other parameters such as the oil refractive index, the light wavelength, the camera-viewing angle and the oil temperature. All these information was needed for further processing of the video camera records to obtain the wall shear stress.

Because of the temperature dependence of the oil viscosity, the silicon oil viscosity has been measured carefully for different temperatures using the capillary-tube viscometer with an accuracy better than ±2.5%.

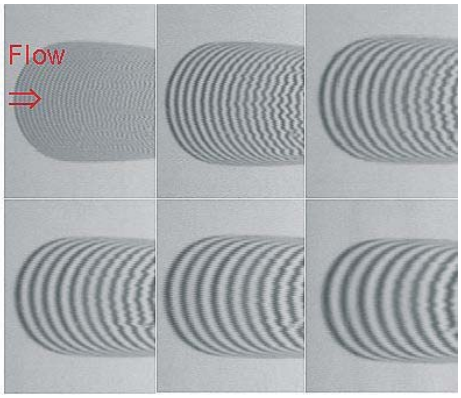

Fig. 6 Image stacks of oil film showing the development of fringe pattern for a constant wall shear stress.

2.4. Hot-film anemometer

A Dantec mini-CTA 54N81, Multi-channel constant-temperature anemometer, was used for the hot-film measurements with overheat ratios namely a=0.2:0.4, here a is defined as $a=(R_w-R_a)/R_a$, where R_w is the operational hot-film resistance and R_a is the film resistance at ambient air temperature, or "a" can be also defined as $a=\Delta T/T_a$, where $\Delta T=(T_f - T_a)$, T_f is the film temperature, and T_a is the ambient air temperature. The sensor is a flush-mounting probe obtained from Dantec Dynamics. The sensing element of the HFA is made of a thin Nickel film deposited on a 50 μm thick Kapton foil. The film is 100 μm wide with an effective length of 0.9 mm and connected to gold-plated lead (Fig. 7). It has a resistance of approximately 10 Ω at an ambient temperature of 20 C° and it is usually glued directly onto the wall where measurements to be carried out. The surface hot film was in situ-calibrated against the data obtained either from the LDA system (DANTEC Flowlite) or the OFI technique.

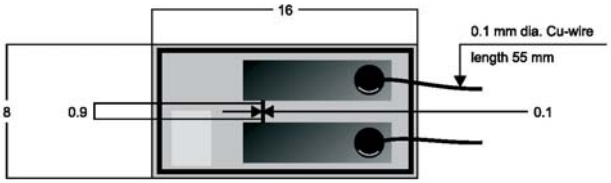

Fig. 7 The DISA 55 R47 hot-film sensor, extracted from Dantec Dynamic.

Basically, the principal of the hot film sensor is based on the analogy between the local wall shear stress and the heat loss from the sensing element. The heat loss is then correlated to the wall shear stress by the power law (i.e., King's Law):

$$E^2 = A + B\,\tau_w^{1/3} \quad (4)$$

where A, and B are constants determined by calibrating the hot film against the LDA or the OFI techniques, E and τ_w are the time-averaged hot-film output and wall shear stress, respectively. The calibration constants depend on

the flow velocity and temperature, sensor geometry, as well as the wall properties. The heat loss to the substrate suggests that adiabatic walls are to be used and to carry out in situ calibration of the hot-film sensor. Hence, because of the heat loss from the sensing element to the substrate and the feedback of the heat from the substrate to the fluid the above relation, equation (4), might be no longer applicable to expect that the heat loss from the hot film varies with the cube root of the wall shear stress. As a result the above equation can be rewritten as follows:

$$E^2 = A + B\,\tau_w^{\,n} \tag{5}$$

where A, B and n are simultaneously and experimentally determined by a least-squares fit. see, e.g.; [4, 17].

The temperature of the air stream inside the wind tunnel was kept constant during the calibration and the measurements so as to yield accurate hot-film results. However, a correction for temperature drift was carried out in case of an unavoidable temperature change. Nitsche et al. [1984] observed that ±1°C temperature drift results in more than 5% shear stress measuring error.

3. RESULTS AND DISCUSSIONS

Accurate and preferably independent measurement of the wall skin friction with high spatial resolution is needed for reliable investigations of the laminar and the turbulent wall-bounded shear flows. Hence, the present work aims at applying and comparing three different measuring techniques to obtain the wall skin friction in two-dimensional boundary layer flows.

Further, there is a general believe in fluid mechanics community that the inner layers of wall-bounded flows scale with the wall friction velocity, u_τ. There is a common agreement also that the mean velocity distribution in the region close to the wall, i.e., within the viscous sublayer, is given by:

$$\frac{U}{u_\tau} \equiv \frac{y u_\tau}{\nu} \tag{6}$$

Hence, it seems from the first glance that it is easy to determine the wall skin friction velocity by carrying out velocity measurements close to the wall. However, in most aerodynamics applications, the thickness of the viscous sublayer is too thin to obtain accurate velocity information within it, in particular, at high Reynolds number in addition to the effect of the size of the CV of the measuring technique. If the size of the CV of the measuring technique is too large to spatially resolve the laminar sublayer, it is assumed that the logarithmic law of the wall can be employed. Clauser [1954], therefore, constructed his well-known plot based on the logarithmic velocity profile:

$$\frac{U}{u_\tau} = \Lambda \log \frac{y u_\tau}{\nu} + C \tag{7}$$

which can be rewritten as follows

$$\frac{U}{U_\infty} = \sqrt{\frac{c_f}{2}} \left[\Lambda \log\left(\frac{y U_\infty}{\nu} \right) + \Lambda \log\left(\sqrt{\frac{c_f}{2}} \right) + C \right] \tag{8}$$

where $\Lambda \equiv 1/\kappa$, κ is the von Kàrmàn constant and C is the additive constant. The use of the Clauser plot is proposed in the present study since the most recent scaling laws support the logarithmic velocity profile in boundary layer flows, see e.g.; [12-14]. Basically, to obtain a value for the skin friction coefficient c_f utilizing the Clauser method, it is usually superposed on a measured velocity profile and the value of the skin friction coefficient can be obtained by matching both, i.e., equation (8) with the mean velocity experimental data, see Fig. 8.

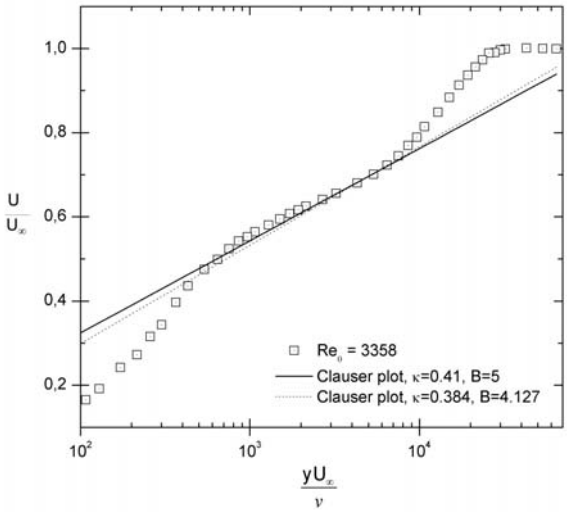

Fig. 8 The Clauser chart superposed on a selected case of the current LDA experimental results.

It is obvious from equation (8) that there is a direct dependence of the skin friction coefficient upon the values adopted for the von Kàrmàn constant, κ, and the additive constant, C. Recent and accurate values for both constants obtained by [12, 14] from boundary layer measurements are utilized resulting in precise application for the Clauser plot when compared with the measuring techniques used in the present study to get the wall skin friction data. The wall skin friction values obtained, utilizing the log line constants either obtained by [12] [Λ=6.059 (κ=0.38), C=4.1] or [14] [Λ=5.996 (κ=0.384), C=4.127] were found to be ±1% in good agreement when the most common values [Λ=5.996 (κ=0.41), C=5.0] adopted by [18] for turbulent boundary layers are to be used, see Fig. 8. It is surprising that the most recent values obtained by [12, 14] are in close agreement with values proposed by [19], Λ=6.05 (κ=0.3806) and C=4.05 a long time ago. It should be also noted that the values utilized with the logarithmic velocity profile are for smooth flat surfaces under zero pressure gradient.

In addition to the LDA and the OFI, the HFA was used to obtain information about the mean wall skin friction as well as flow transition. The heat loss ($\dot{q}$) from the HFA in the wall vicinity, where sheared flow exits, was observed to depend on the wall shear stress, τ_w, or in other words the mean velocity gradient $(d\overline{U}/dy)_w$, the wall thermal conductivity (λ_w) and the overheat ratio $(\Delta T/T_a)$, i.e.,

$$\dot{q} = f\left[\frac{d\overline{U}}{dy}, \lambda_w, \frac{\Delta T}{T_a} \right] \tag{9}$$

The substrate thermal conductivity effect on the hot-film output was documented, therefore, by carrying out experiments, see Fig. 9, over an adiabatic (glass) and a heat-conducting (aluminum) substrates, verifying the

influences of the main parameters expressed in equation (9). Figure 9 indicates, clearly, that the heat loss from the HFA is affected by the substrate thermal conductivity. For a common overheat ratio and under the same values of the wall shear stress, the data indicate the wall conductivity effect on the hot-film readings. In the absence of the flow, the output of the HFA denoted by A in the calibration equation is equal to E_0^2 and as it was expected it has a higher value above the aluminum substrate (A=2.657) when compared with the value obtained above the adiabatic substrate (A=1.894). As a result, the output difference (E^2 - E_0^2) measured above the heat-conducting substrate, i.e., aluminum, are lying under those for the adiabatic substrate (glass) for the same wall shear stress.

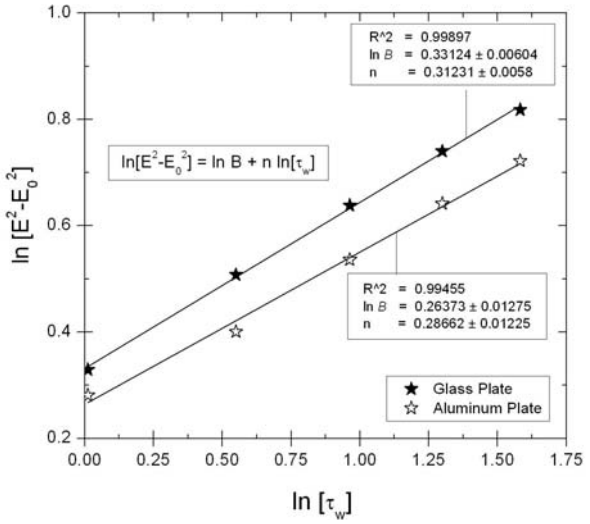

Fig. 9 The hot film output over highly heat-conducting (aluminium λ_w=220 W/m K) and adiabatic (glass λ_w=0.8 W/m K) substrates for the same overheat ratio, a=0.4.

One more important parameter, which has to be taken into further consideration, was that choosing the appropriate material to glue the hot-film sensor to the substrate [20].

Considering the normalized heat transfer from the HFA as follows:

$$\rho^* c_p^* \frac{\partial T^*}{\partial t^*} = \lambda^* \frac{\partial^2 T^*}{\partial x_i^{*2}} \left[\frac{\lambda_c t_c}{\rho_c c_{pc} l_c^2} \right] \qquad (10)$$

$$t_c = \frac{l_c^2}{\alpha_c}, \quad where \quad \alpha_c = \frac{\lambda_c}{\rho_c c_{pc}}$$

clarifies the substrate thermal conductivity effect on the HFA readings. Here c_p stands for the specific heat of the substrate at constant pressure, ρ is the density of the substrate, t_c is the characteristic conduction time scale, and l_c is the characteristic length scale.

For the two different substrates (i.e., aluminum and glass) with the same characteristic length scale, l_c, the ratio of the heat conduction time scale for the aluminum to the glass is equal to the inverse ratio of the two thermal conductivities. This indicates that the substrate of high conductivity absorbs heat more and faster than the adiabatic substrate and explains the differences between the HFA readings over the conducting and the adiabatic substrates shown in Fig. 9. In addition, in the wall vicinity, small velocities exist, and therefore the heat loss by free convection is not dominant since Gr<Re^3 [21], and thus for constant Pr, most of the heat went into the substrate because of the heat diffusion, term (II) in equation (11) that represents the normalized thermal energy equation, expressing the heat transport to the substrate:

$$\underbrace{U_i^* \frac{\partial T^*}{\partial x_i^*}}_{I} = \underbrace{\left[\frac{1}{\mathrm{Re\,Pr}} \right] \lambda^* \frac{\partial^2 T^*}{\partial x_i^{*2}}}_{II} + \underbrace{\left[\frac{Ec}{\mathrm{Re}} \right] \phi^*}_{III} \qquad (11)$$

Therefore, it might be concluded that the diffusivity is dominant and mainly responsible for the heat loss from the HFA rather than the free convection.

A summary of the wall skin friction data obtained from all three measuring techniques, i.e., the LDA, the OFI as well as the HFA is presented in Fig. 10 for the smooth surface boundary layer flows for $Re_x \leq 2\times10^6$.

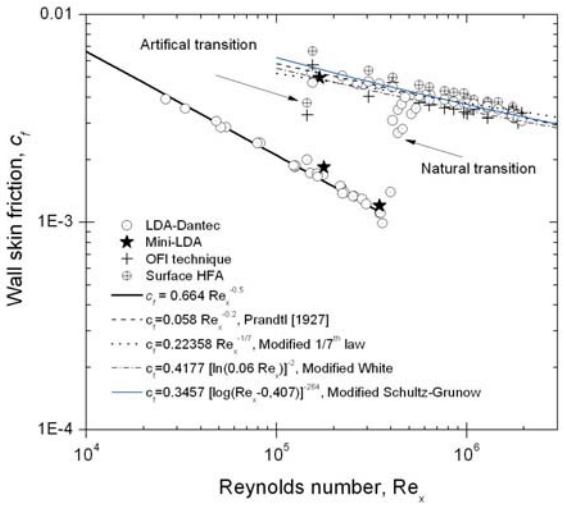

Fig. 10 Summary of the wall skin friction results compared with laminar and turbulent formulae extracted from the literature.

It is worth noting that the wall skin friction data obtained using the LDA near-wall mean velocity profile has been carried out applying the stress-strain relation. i.e., equation (1) when reliable velocity data within the viscous sublayer were obtained, in particular, for the laminar flow cases. On the other hand, for the turbulent flow cases, the computations of the skin friction values were carried out utilizing the Clauser method.

Fig. 10 compares, therefore, the wall skin friction data from the three measuring techniques. The surface hot-film was observed to overestimate the wall skin friction data, indicating that the thermal conductivity of the substrate and the glue material influence to a great deal the heat loss from the HFA for reasons mentioned above. On the other hand, a satisfactory agreement was obtained between the wall skin friction data obtained from the OFI and the LDA near-wall mean velocity profile. However, one can observe small under estimation of the OFI data shown in the figure that might be attributed to the accuracy of the oil viscosity measurements and/or the temperature of the wall surface where measurements have been carried out. Various modified curves by [14],

representing the wall skin friction relations have been fitted to the current experimental data in the figure, showing good agreement, in particular, the modified Schultz-Grunow relation as well as the Prandtl power law. Some preliminary wall skin friction results using the mini LDA have been also presented, see [22] for more details.

4. CONCLUSIONS

The analysis of the present results indicate that the evaluation of the wall skin friction data utilizing the Clauser method is applicable with appropriate values for both constants of the log line and when accurate velocity data within the logarithmic layer are obtained.

The thermal conductivity of the substrate plays a major role in the heat loss from the HFA, and therefore, the heat diffusivity is dominant and responsible for its heat loss rather than the free convection. The Kapton film although it has a low thermal conductivity it is still not an effective heat-insulating material. Additional measurements are to be carried out for better understanding of the substrate and glue effects on the HFA performance.

The above discussions and the good agreement of the preliminary results obtained using the mini-LDA versus the three measuring techniques utilized here encouraged the authors to further develop the mini-LDA compined with a HFA array in one module in co-operation with Astro- und Feinwerktechnik Adlershof GmbH and TFH Wildau.

ACKNOWLEDGMENTS

The grant of German Luftfahrtforschungsprogramm (LuFo 3) FKZ 20F0301A, to carry out the present work is gratefully acknowledged and the help from both Astro- und Feinwerktechnik Adlershof GmbH and University of Applied Sciences Wildau (TFH Wildau).

REFERENCES

[1] V. I. Kornilov, “Reduction of turbulent friction by active and passive methods (Review),” Thermophysics and Aeromechanics 2005, Vol. 12, No. 2, pp. 175-196.

[2] L. H. Tanner, and L. G. Blows, “A study of the motion of oil films on surface in air flow, with application to the measurements of skin friction," J. Phys. E 2, 3, pp. 194-202, boundary layers," Prog. Aerospace Sci. 1976, 18, pp. 1-57.

[3] K. G. Winter, “An outline of the techniques available for the measurement of skin friction in turbulent boundary layers,” Prog. Aerospace Sci. 1977, Vol. 18, pp. 1-57.

[4] W. Nitsche, C. Haberland, and R. Thünker, “Comparative Investigations on friction drag measuring techniques in experimental aerodynamics,“ 14th Congress of the Int. Council of the Aeronautical Sciences, September 9-14, 1984, Toulouse, France, pp. 391-403.

[5] F. Durst, H. Kikura, J. Jovanovic, and Q. Ye, “Wall shear stress determination from near-wall velocity data in turbulent pipe and channel flows, ," Exp. Fluids 1996, Vol. 20, pp. 417-428.

[6] F. Durst, E.-S. Zanoun, and M. Pashtrapanska, “In situ calibration of hot wires close to highly heat-conducting walls," Exp. Fluids 2001, Vol. 31, pp. 103-110.

[7] H. H. Fernholz, G. Janke, M. Schober, P- M. Wagner, and D. Warnack, “New developments and applications of skin-friction measuring technique," Meas. Sci. Tech. 1996, Vol. 77, pp. 1396-1409.

[8] F. Durst, and E.-S. Zanoun, “Experimental investigation of near-wall effects on hot-wire measurements," Exp. Fluids 2002, Vol. 33, pp. 210-218.

[9] J. D. Ruedi, H. Nagib, J. Österlund, and P. A. Monkewitz, “Evaluation of three techniques for wall-shear measurements in three-dimensional flows,” Exp. Fluids 2003, Vol. 35, pp. 389-396.

[10] E.-S. Zanoun, H. Nagib, and F. Durst, “Refined Cf relation for turbulent channels and consequences for high Re experiments,” Fluid Dyn. Res. 41 (2009) 021405, pp. 1–12.

[11] F. H. Clauser, “Turbulent boundary layers in adverse pressure gradients,“ J. Aeronaut. Sci. 1954, 21, pp. 91-108.

[12] J. M. Österlund, A. V. Johansson, H. M. Nagib, and M. H. Hites, “Wall shear stress measurements in high Reynolds number boundary layers from two facilities," 30th AIAA 99-3814, Fluid Dynamics Conf 1999.

[13] E.-S. Zanoun, F. Durst, and H. Nagib, “Evaluating the law of the wall in two-dimensional fully developed turbulent channel flows,” Phys. Fluids 2003, Vo. 15, pp. 3079-89.

[14] H. M. Nagib, K. A. Chauhan, and P. A. Monkewitz, “Approach to an asymptotic state for ZPG turbulent boundary layers,” Phil. Trans. Royal Soc. A 2007: Scaling and structure in high Reynolds number wall-bounded flows 95, pp. 755-770.

[15] M. Kito, E.-S. Zanoun, L. Jehring, and C. Egbers, “Laser-Doppler anemometry in turbulent boundary layers induced by different tripping devices compared with recent theories,” Fachtagung "Lasermethoden in der Strömungsmesstechnik" GALA e.V.; 5-7 September 2006, Braunschweig, Germany

[16] C. Bourassa, F. O. Thomas, and R. C. Nelson, “Experimental investigation of turbulent boundary layer relaminarization with application to high-lift systems: preliminary results,” AIAA Paper, 2000, pp. 4017.

[17] R. J. Goldstein, “Fluid Mechanics Measurements," Hemisphere Publishing Corporation, NY, 1983.

[18] Computation of turbulent boundary Layers-1968, Proceeding of AFOSR–IFP–Stanford Conference, Vol. 2, edited by D. E. Coles and E. A. Hirst, Thermosciences Div., Dept. of Mechanical Engineering, Stanford Univ., Stanford, CA, 1969.

[19] K. G., Winter, and L. Gaudet, “Turbulent boundary-layer studies at high Reynolds numders at Mach numbers between 0.2 and 2.8,” ARC R & M 3712, 1970.

[20] E.-S. Zanoun, C. Egbers, L. Jehring, “Modified Optical and Thermal Anemometers for Laminar and Turbulent Boundary Layers Investigations,” 4th International Conference on Heat Transfer, Fluid Mechanics and Thermodynamics, HEAT2005, September 19 th –22nd, 2005, Cairo, Egypt.

[21] D.C. Collis, M.J. Williams, “Two-dimensional convection from heated wires at low Reynolds numbers, J. Fluid Mech. 1959, Vol. 6, pp. 357–384.

[22] L. Jehring, E.-S. Zanoun, C. Egbers, S. Eckert, C. Schultz, and D. Suchland, “Fortschritte bei der Entwicklung und Anwendung eines miniaturisierten Sensors für wandnahe Strömungen,” In: 13. “Fachtagung Lasermethoden in der Strömungsmesstechnik“, GALA e.V.; 6-8 September 2005, Cottbus, Germany.